Search for Disease-Causing Variants in Families with Postaxial Polydactyly Using Whole Exome Sequencing.

by

Palwasha Iqbal

Department of Biochemistry
Faculty of Biological Sciences
Quaid-i-Azam University Islamabad, Pakistan
2023

Search for Disease-Causing Variants in Families with Postaxial Polydactyly Using Whole Exome Sequencing.

A thesis submitted in partial fulfilment of the requirements for the degree of Master of Philosophy

in

Biochemistry & Molecular Biology

by

Palwasha Iqbal

Department of Biochemistry
Faculty of Biological Sciences
Quaid-i-Azam University Islamabad, Pakistan
2023

Dedicated to My Loving Family for Their

Endless Love, Support and Prayers.

Quaid-i-Azam University, Islamabad, PAKISTAN
Department of Biochemistry
Faculty of Biological Sciences

CERTIFICATE

This thesis, submitted by **Ms. Palwasha Iqbal** to the Department of Biochemistry, Faculty of Biological Sciences, Quaid-i-Azam University, Islamabad, Pakistan, is accepted in its present form as satisfying the thesis requirement for the Degree of Master of Philosophy in Biochemistry/Molecular Biology.

Examination Committee:

1. **External Examiner:**
   Dr. Samreen Saleem
   Associate Professor
   Department of Public Health,
   Nutrition & Life style Medicine,
   Health Services Academy, Islamabad
   Signature: _____

2. **Supervisor:**
   Dr. Imran Ullah
   Signature: _____

3. **Chairperson:**
   Prof. Dr. Iram Murtaza
   Signature: _____

Dated: **October 25, 2023**

Declaration

I hereby declare that the work presented in this thesis is my own effort and hard work. It is written and composed by me. No part of this thesis has been previously published or presented for any other degree or certificate.

Palwasha Iqbal

Table of Contents

Acknowledgements

All the praise and thanks be to **ALLAH**, to Whom belongs all that is in Heavens and that is in the earth, and to Him belongs all praise in the Hereafter. And He is the Wise, the Acquainted. I offer my utmost regards, respect, and blessings to the Holy Prophet **Hazrat Muhammad (SAW)** whose teachings have profoundly enriched my thoughts and ambitions.

I must express my profound appreciation to my supervisor, **Assistant Professor Dr. Imran Ullah**, of the Department of Biochemistry in the Faculty of Biological Sciences at Quaid-i-Azam University Islamabad, for his unwavering guidance and supervision during this research. Furthermore, I extend my thanks to **Dr. Irum Murtaza**, Chairperson of the Department of Biochemistry, for her unrelenting dedication to fostering research activities in the department. Also, I want to express my gratitude to **Prof. Dr. Wasim Ahmad,** for helping and guiding us in the research activities in the laboratory.

I would like to express my sincere gratitude to **Dr. Abdullah** and **Kifayat Ullah** for their invaluable cooperation, guidance, support, and suggestions, which had a tremendous impact on my research work. Their contributions were pivotal in making my research a success. Without their help, my work would have been very difficult. I express my gratitude to **Hajira Fayyaz, Fatih Ullah, and Hammal Khan Zehri** for their unwavering guidance and support throughout my research. I must appreciate the friendly and cooperative attitude of my lab seniors **Dr. Attieya Zaman, Amjad Tanoli**, **Aamir Sohail, Javed Khan, Sohail Ahmed, Inam Banochi, Tahir, Maria Taj, Zumar Fatima** and **M. Ilyas.**

I am extremely thankful to my classmates **Irum Nasir, Mirub Chaudhry and Murtaza Hasnain** for their moral support throughout my research journey. I am truly grateful for their friendship and assistance. Their unwavering encouragement and insightful discussions greatly enriched my research experience.

I am also thankful to my lab **juniors Arooba, Ayesha Sani, Rehmat Ullah, Raza Sufyan** and **Sher Aziz** for the respect they gave to me. I present my heartiest thanks

to friends **Wishma Seher, Alina Murtaza** and **Syed Hamid Abbas** for their constant moral support throughout my academic journey.

I must express my heartfelt gratitude to **my family**, with a special mention to my beloved mother **Kaneez Fatima**, my father **Zafar Iqbal**, my loving sister **Kanwal Iqbal** and my cherished brothers **Muhammad Sohail** and **Muhammad Shahzaib**. Their unwavering support, boundless encouragement, and well wishes have been the driving force behind my achievements. The continuous stream of prayers, affection, and guidance from my parents and siblings has undeniably been the cornerstone of my journey to success.

Lastly, I extend a sincere acknowledgement to **myself** for maintaining unwavering self-belief during the most challenging phases of my academic journey. My tenacity and self-confidence have been pivotal in surmounting obstacles, making this journey of growth and learning more remarkable.

PALWASHA IQBAL

LIST OF FIGURES

LIST OF TABLES

LIST OF ABBREVIATIONS

AD	Autosomal Dominant
AR	Autosomal Recessive
AMD	Acromesomelic Dysplasia
AER	Apical Ectodermal Ridge
BBS	Bardet-beidl Syndrome
BCC	Basal Cell Carcinoma
CED	Camaurati Engelman Disease
CFAP	Cilia and Flagella Associated Protein
CNV	Copy Number Variation
CRD	Cysteine-rich Domain
CRJS	Curry–Jones syndrome
CZIB	CXXC Zinc Binding motif Protein
DACH1	Dachshund Family Transcription Factor 1
DNA	Deoxyribonuclease
EB	Elution Buffer
ECD	Extracellular Domain
EDTA	Ethylene Diamine Tetraacetate
EtBr	Ethidium Bromide
EVS	Ellis-Van Crevald Syndrome
FGF	Fibroblast growing factor
GATK	Genome Analysis Tool kit
GCPS	Greig Cephalo-Polysyndactyly Syndrome
GSD	Genetic Skeletal Dysplasia
HEC	Higher Education Commission
HGMD	Human Genome Mutation Database
HOX	Homeobox gene
IFSSH	The International Federation of Societies

	for Surgery of Hand
IQCE	IQ Motif containing E
IRB	Institutional Review Board
LMBR1	Limb Development Membrane Protein 1
MB	Medulloblastoma
MSC	Mesenchymal stem cell
OD	Optical Density
PAP	Postaxial Polydactyly
PAP-A	Postaxial Polydactyly Type A
PAP-B	Postaxial Polydactyly Type B
PCR	Polymerase Chain Reaction
PPD	Preaxial Polydactyly
PHS	Pallister-Hall Syndrome
Rpm	Rotation Per Minute
SHFM	Split Hand and Foot Malformation
SHH	Sonic Hedgehog
SMO	Smoothened
SNV	Single Nucleotide Variant
TBE	Tris-Borate EDTA
TE	Tris EDTA Buffer
TGF- β	Transforming Growth Factor Beta
TMPPE	Transmembrane Protein with metallophosphoterase domain
TPT	Tri-phalangeal Thumb
RA	Retinoic Acid
GLI3	Gli Family Zinc Finger 3
WB	Wash Buffer
WES	Whole Exome Sequencing

WNT	Wingless-type MMTV integration site family
YCGA	Yale Centre for Genome Analysis
ZNF	Zinc Finger Protein
ZPA	Zone of the Polarising Activity

ABSTRACT

Polydactyly, also known as hexadactyly or hyperdactyly, is a genetic limb disorder characterized by the presence of an extra digit. Polydactyly can be inherited in autosomal dominant or recessive form and has syndromic and non-syndromic types. Postaxial polydactyly (PAP) refers to one or more additional digits at the ulnar/fibular side of the hand/foot respectively. In the current study, the families were identified with the Non-Syndromic Postaxial Polydactyly and proceeded with the molecular and clinical analysis in order to find a potential candidate gene.

Family A showing an autosomal dominant inheritance pattern in the consanguineous family was followed for WES. The WES followed by Sanger sequencing was performed to identify the potential disease-causing variant. These variants were also scrutinised by various *in-silico* tools. WES analysis of family A revealed a novel variant (exon 13, c.1657G>A; p.555Val>Met) of *FGFR3*, mapped on chromosomal position 4p16.3, in isolated bilateral PAP in lower appendages. Family B exhibits an autosomal recessive inheritance pattern in the non-consanguineous family. The WES followed by Sanger sequencing identified a novel homozygous missense mutation (c.1792G>A; p.598Gly>Arg) in exon 10 of the already reported *SMO* gene in non-syndromic PAP. In conclusion, the present research study identified two variants that might help better understand genotype-phenotype correlation. This study will help in the understanding of the role of *FGFR3* and *SMO* in limb deformities and will also help in the prenatal testing and genetic counselling of the affected families.

Chapter 1
INTRODUCTION

INTRODUCTION

The skeleton is an intricate network of bones, cartilage, ligaments, joints, and tendons. The adult skeleton is composed of bone, hard dense connective tissue. The skeleton provides shape and support to our body as well as protection for various body organs (the heart, lungs, brain, spinal cord, kidneys). It also maintains acid-base balance and mineral homeostasis, stores and releases fats and bone marrow harbours niches for hematopoiesis (Taichman, 2005). In addition, it also plays a role in endocrine regulation (Blottner *et al.,* 2008).

A human skeletal system is an endoskeleton, made up of hard, mineralized components embedded inside soft tissues. In the vertebrate embryo, ectoderm and mesoderm produce multipotent mesenchymal cells that migrate to particular parts of the body and begin the process of skeletogenesis (Erlebacher *et al.,* 1995). The embryonic cells continue to differentiate into three distinct cell types, chondrocytes, osteoclasts, and osteoblasts. The skeletogenic cells then initiate osteogenesis (the production of bones) through two processes: endochondral ossification and intramembranous ossification. The endochondral bone formation is responsible for the growth of long bones while the bones of the craniofacial skeleton and some of the clavicle are generated by intramembranous ossification (Zelzer and Olsen, 2003).

Human Skeletal Architecture

The Human skeleton is comprised of 206 bones (which have 126 appendicular, 74 axials and 6 ossicle bones), cartilages and joints.

The size and shape of the skeleton depend upon the positioning and patterning of skeletal elements called patterning factors (Savarirayan and Rimoin, 2002). These patterning factors include cells from three differentiating embryonic lineages comprising somites, lateral plate mesoderm and the neural crest. As soon as the pattern develops, the mesenchymal precursor cells relocate to the site of skeletogenesis, where these cells condense and then differentiate. Mesenchymal condensation is involved in the direct formation of bones without the involvement of cartilage intermediate (Crombrugghe *et al.,* 2001). Different forms of bones, including short bones (wrist, ankle), long bones (femur, humerus), flat bones, irregular bones,

and sesamoid bone forms, depends on the dimensions, size, shape, and number of cartilage templates (vertebrae) (Kornak *et al.,* 2003).

Limb Development

Limbs are appendages that play an important role in communication, locomotion, and other intricate processes. The precise shape and positioning of bones and joints are made possible by a complex interaction of several elements during the formation of the vertebrate limb skeleton (Waldmann *et al.,* 2022). Four phases of limb development are involved: the construction of the limb field, the generation of specific point signals that design the field, the record-keeping of positional information in a field as specific gene expression and lastly, the controlled differentiation of the limb anatomy based on the positional information that has been encoded (Johnson and Tabin, 1997).

Proliferating mesenchymal cells are important in limb outgrowth; these cells begin to differentiate from the proximal to the distal end (humerus to digits) and from the anterior to the posterior end (first to a fifth digit) of the limb as it grows (Capdevila and Belmonte, 2001). Vertebrate limb development is influenced by the number of genes and pathways. Homeobox genes like *HOXA11, HOXA13,* and *HOXD13* contribute to the initial patterning of cartilage in the development of the limbs. The *HOX* code contributes to the positioning of the limb field in vertebrates. The canonical *WNT* pathway also known as the *β*-catenin pathway, plays a role in the development of both the hind limbs and the forelimbs. Retinoic acid (RA) and *FGF* pathways (*FGF2, FGF8,* and *FGF10*) are also involved in the particular limb patterning process. The proximal stylopod, distal autopod, and zeugopod are three major zones for vertebrate limb development. The apical ectodermal ridge (AER), zone of the polarising activity (ZPA), and dorsal ectoderm are key players in regulating a patterning in the anteroposterior (A/P) axis, proximal to distal projection, and establishing dorsoventral polarity respectively. Sonic Hedgehog (SHH) regulates the activity of ZPA and an outgrowth of limb ectoderm. In digit formation, the identity and number of digits are mediated by SHH (Capdevila and Belmonte, 2001). *GLI3* and SHH both show expression in limb development. The role of SHH and *GLI3* in vertebral limb development was determined in mice by gene knockout. With

the exception of one rudimentary digit, all others were lost in mutant mice. Mutation in SHH and *GLI* in humans leads to several skeletal disorders like pre-axial and post-axial polydactyly (Hong *et al.,* 2012).

Skeletal Pathways

Bone formation and skeletal patterning is a tightly regulated process in the presence of several patterning transcription factors like *RUNX2, SOX9,* and bone signaling pathways including Sonic hedgehog (SHh), Fibroblast growth-factor *(FGF),* Wingless/integrated *(Wnt),* Notch, and the Bone morphogenetic proteins *(BMPs)* (Lefebvre and Bhattaram, 2010).

- **The FGF Signaling Pathway**

Fibroblast growth-factors *(FGFs)* are categorized into a family of 22 proteins that along with sulphated glycosaminoglycans (GAGs) such as heparin results in the activation of Fibroblast growth-factor receptors *(FGFRs)* (L'Hôte and Knowles, 2005). *FGFRs* are made up of a cytoplasmic domain with protein tyrosine kinase activity, one transmembrane helix domain, and an extracellular ligand binding protein region comprising three immunoglobulins (ig) like domains (D1-D3) (Schlessinger *et al.,* 2000). The *FGFR* dimerizes upon binding the FGF proteins and stimulates tyrosine kinase receptors and autophosphorylation of the cytoplasmic domain. Various signal transducers then bind to the auto-phosphorylated site which causes the *RAS* oncogene to be recruited. *RAS* then further activates the MAP kinase (MAPK), dual specific MAP kinase pathway via ERK (MAPKK), phosphoinositide 3-kinase AKT, and ser/thr kinase Raf signaling cascades. These proteins stimulate genes involved in cell proliferation and division (Boilly *et al.,* 2000; Yamada *et al.,* 2004).

Aberrant *FGF* signaling leads to congenital syndromes and skeletal dysplasia such as achondroplasia, craniosynostosis, polydactyly, and deafness (Teven *et al.,* 2014).

- **The Hedgehog Signaling Pathway**

Hedgehog (Hh) is a protein that acts as a morphogen that is secreted and released in the paracrine signaling pathways. Hedgehog consists of three homologues; Desert Hedgehog (DHh), Indian Hedgehog (IHh), and Sonic Hedgehog (SHh). SHh plays a crucial role in facilitating the growth and patterning of developing limbs and is

expressed in the notochord, neural tube, and ZPA of the developing limb bud (Lopez-Rios, 2016). SHh is reported to involve in the development and maintenance of skeletal tissues and in the production of the growth plate and joint formation. Major components of the SHh pathway are *SMO, PTCH,* and *GLI* transcription factors (Xavier *et al.,* 2016). The Smoothened *(SMO)* is a seven-transmembrane receptor protein along with Patched (PTCH), a 12-transmembrane protein to which SHh binds as a ligand (Riobo *et al.,* 2006). When the SHh is not bound, *PTCH* suppresses *SMO* activity, causing *SUFU* to bind to the *GLI* transcription factor and is degraded by proteasome upon phosphorylation by *GSK3β, CK1,* and *PKA*. *GLI* converts to *GLIr* and travels to the nucleus to prevent the downstream target genes from being transcribed. *SMO* inhibition is relieved while SHh is present as it binds to the PTCH. The activated *SMO* then prevents the degradation of *GLI* by preventing its sequestration from SUFU and phosphorylation from *GSK3β, CK1,* and *PKA*. The activated *GLI* (GLIa) then translocate to the nucleus and acts as a transcription factor for various SHh target genes (RUNX2, OSX) which then differentiate into osteoblasts (Fig. 1.1) (Salhotra *et al.,* 2020; Fan *et al.,* 2022).

The hedgehog pathway interacts with other signaling pathways like Wnt and BMPs and is crucial for the formation of the skeleton. The dysregulated hedgehog pathway leads to various skeletal anomalies, such as osteoporosis, osteoarthritis, syndactyly, and polydactyly (Long and Ornitz, 2013).

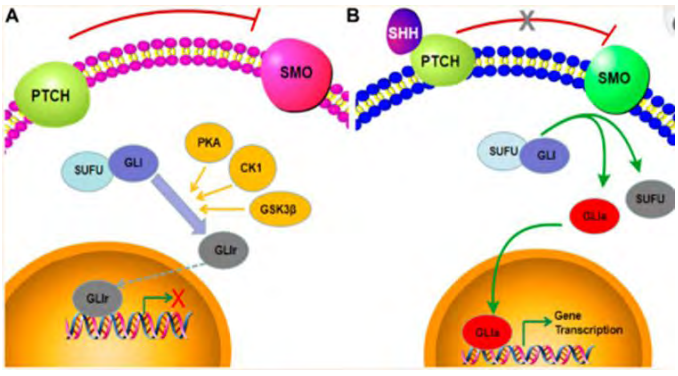

Fig. 1.1. Graphical presentation of SHh-mediated signaling pathway. **(A)** In the absence of SHh, SMO is inhibited by PTCH. **(B)** In the presence of SHh, it binds to the PTCH and activates SMO (Fan *et al.,* 2022).

- **The Wnt Signaling Pathway**

Wnts are a large family of secreted glycoproteins that intracellular signaling classifies into three diverse pathways: (1) the gene regulation regulated by the *Wnt* Canonical pathway/β-catenin pathway, (2) the gene regulation controlled by non-canonical Wnt pathway that involves Jun N-terminal kinase (JNK), and (3) the Wnt/Calcium pathway. The wnt/β-catenin pathway is activated when *Wnt* binds to the extracellular cysteine-rich region (domain) of the 7 transmembranes frizzled (Fzd) receptor and the *LRP5/6* co-receptor. When the *Wnt* is absent, cytoplasmic *β-catenin* is shattered by phosphorylation of the combined action of serine/threonine glycogen synthase kinase-3β *(GSK-3β)* and a multiprotein complex axin, APC, and diversin (Huelsken and Behren, 2002).

While in its active state, *Wnt* binds to the Fzd and its co-receptor (LRP5/6) to activate the β-catenin pathway. Dishevelled (Dsh) is activated, which blocks a *β-catenin* degradation complex. When *β-catenin* is stabilized, it penetrates into the nucleus, forms an association with *TCF/LEF* transcription factors and activates the *Wnt* target genes transcription. The aberrant *Wnt* signaling pathway leads to many skeletal disorders (Holstein, 2012)

- **The BMP Signalling Pathway**

The Bone morphogenetic proteins (BMP) are secreted glycoproteins belonging to a *TGF-β* superfamily and their signaling has also been linked to several developmental events in embryos and adults. It regulates numerous skeletal developmental processes including mesoderm differentiation, osteoblast and chondrocyte proliferation, joint formation and tooth development, and cartilage and bone development through a series of signaling cascade events. BMPs are also involved in limb development (Wan and Cao, 2005). There are over 20 different types of BMPs and are known to involve in the osteoblastic differentiation of MSCs. Depending on their specificity of interaction with different receptors, some may have overlapping functions while other acts individually. Two types of the serine/threonine protein kinase receptors (type I and type II), and various members of SMAD family transcription factors transmit BMP signals to the nucleus (Massagué and Chen, 2000). Type I receptor have further three different receptors (Alk2, Alk3, and Alk6) while type II have only one BMP

receptor (BMPrII). Type I receptor is phosphorylated which leads to its activation by the BMP ligand's binding to the type II receptor, which then results in phosphorylation of the BMP pathway specific receptor-regulated SMADs (R-SMAD). Two R-SMADs then bind to the SMAD-4 to form the heterotrimeric complex that propagates into the nucleus to control the expression of the BMP target genes (Zhang *et al.,* 2005).

Heterozygous and homozygous loss of function mutation of the BMP pathway lead to many skeletal disorders like brachydactyly (type A1, A2, and D), Osteoporosis, Acromesomelic dysplasia etc (Ahmad *et al.,* 2022).

- **The Notch Signaling Pathway**

During embryonic and postnatal development, Notch is known to control many stem cell fates like differentiation, proliferation and self-renewal. The Notch signaling pathway also shows expression in the development of the skeleton in adult organisms. After a fracture, Notch signaling has been shown to influence bone remodeling and regeneration processes (Wang *et al.,* 2022). Notch receptor has four types (Notch 1-4) and has one intracellular (NICD), one transmembrane, and an extracellular domain (NECD). Its signaling pathway is regulated by an interaction of Notch receptors and their ligands (jagged 1 & 2, and delta-like 1, 3, & 4) expressed on neighboring cells. The NECD of receptors and ligands contain *EGF* repeats that help in their binding. Several other proteins like γ-secretase and metalloprotease (ADAM10) bind to *EGF,* which as a result cleaves and releases NICD into the cytoplasm. The cleaved NICD then moves into the nucleus and monitors the transcription of genes targeted by Notch involved in skeletal development (Ballhause *et al.,* 2021).

Notch signaling inhibition results in abnormalities in cartilage development, poor bone growth, and reduced bone mass. In addition, skeletal abnormalities such as Spondylocostal dysostosis and Alagille syndrome have been linked to mutations in the Notch signaling pathway (Chien *et al.,* 2020).

Genetic Skeletal Dysplasia

Skeletal dysplasias are a genetically complex group of disorders that impact the growth, maintenance and development of the human skeleton. Skeletal dysplasia

refers to generalized skeletal malformations that primarily affect bone (osteodysplasias) and cartilage (chondrodysplasias), hence also known as osteochondrodysplasias. The malformation of single bone or group of bones is known as dysostoses. Genetic skeletal disorders are classified into either nonsyndromic (isolated) or syndromic (complex syndromes) forms and are inherited in autosomal dominant or recessive, X-linked or *de novo* forms (Abbas *et al.,* 2023, Baldridge *et al.,* 2010).

A number of revisions were published by Nosology that classified various skeletal disorders and the genes responsible for them into the groups of disorders, first on the basis of radiographic criteria, then by metabolic criteria, and finally by molecular and functional criteria. The "Nosology of the genetic skeletal disorders" has undergone its 11th revision in 2023. According to its latest nosology classification, 552 genes are responsible for 771 well-characterized skeletal disorders, each having its own unique MIM number (its online version OMIM). These skeletal disorders are categorized into 41 different groups compared to the previous revision containing 42 groups. Several amendments were made to the current nosology. Numerous groups were renamed. 'Osteopetrosis and related osteoclast disorders' have replaced the term 'Osteopetrosis and related disorders'. The terms brachydactyly without extra-skeletal anomalies and brachydactyly with extra-skeletal manifestations have been replaced with the 'isolated brachydactylies' and 'brachydactylies as a part of syndromes' respectively. 'Split Hand and Foot without and with skeletal manifestations' have replaced the term 'Ectrodactyly without or with other skeletal manifestations'. The existing Nosology has added a new group named as 'Skeletal disorders of para-thyroid hormone signaling cascade' (Unger *et al.,* 2023).

The Nosology also demonstrates the complexity of a human genome as illustrated by the immense number of genes and gene products associated with skeletal development and growth. Skeletal disorders have a molecular and biochemical genetic basis. The biochemical defect has been reported in only a few skeletal disorders, including peroxisomal disorders, certain mineralization maladies, and lysosomal storage diseases. The molecular pathogenic classification of skeletal dysplasia is categorized into

multiple types, like defects in; metabolic pathways, extracellular structural proteins, hormones, receptors, growth factors, transcription factors, nuclear proteins, cytoskeletal proteins, and degradation defects of macromolecules (Rimoin *et al.,* 2007).

A broad range of signalling cascades such as; *TGF-β, FGF, Notch, BMP, WNT,* and Hedgehog pathways are involved in human skeletal system development and any primary or any secondary deregulation of these mechanisms/pathways results in osteochondrodysplasias. Mutation in the member of the transforming growth-factor *(TGF-β)* signaling cascade, *TGF-β1* results in Camaurati Engelman Disease (CED) and the mutations in SOST, a member of the *WNT* pathway cause sclerosteosis. The mutation in *FGF* signaling pathway member *FGFR3* can result in the chondrodysplasias such as hypochondroplasia, thanatophoric dysplasias, and achondroplasias (Baldridge *et al.,* 2010).

Hand and foot patterning anomalies are common types of limb skeletal dysplasias such as osteogenesis imperfect (OI), acromesomelic dysplasia (AMD), split hand and foot malformation (SHFM), bardet-beidl syndrome (BBS), brachydactyly, camptodactyly, syndactyly, and polydactyly. According to the 11th Nosology revision, the prevalence of upper congenital limb deformities ranges from 1 in 500 to 1 in 1000 live births (Abbas *et al.,* 2023).

Polydactyly

The word ‘Polydactyly’ comes from ‘Poly’ refers ‘many’ and ‘dactylos’ refers ‘digits’, which refers to the development of extra/multiple digits, toes or other complicated digital parts. Polydactyly is also termed as ‘hyperdactyly’ or ‘hexadactyly’. It is known to be caused by limb development abnormalities, especially in the patterning and modeling of the growing limb bud. Polydactyly is the most prevalent congenital limb disorder noticed immediately after birth and can take many forms, such as full or partial digit duplication. It affects males twice as frequently as females, with an estimated prevalence of 1.6 to 10.7 per 1,000 in the general population and 0.3 to 3.6 per 1,000 in live births. Polydactyly has a high tendency to affect the upper extremities more so than the lower ones, right hand more so than the left, and the right

foot is less affected than the left one. It is divided into symmetrical or asymmetrical, unilateral or bilateral polydactyly.

Classification of Polydactyly

Polydactyly can be inherited in both non-syndromic (isolated) and syndromic (complex) forms.

1 Non-Syndromic Polydactyly

Non-syndromic polydactyly is further classified as Preaxial Polydactyly (PPD), Mesoaxial/Central Polydactyly, and Postaxial Polydactyly (PAP). PAP is more prevalent as compared with PPD and mesoaxial is a quite rare type. The International Federation of Societies for Surgery of Hand (IFSSH) in 1995 named pre and post-axial polydactyly as radial and ulnar polydactyly respectively. When the thumb is affected, the condition is referred to as radial polydactyly, whereas ulnar polydactyly affects the little finger. When the index, middle, or radial finger is affected it is referred to as central polydactyly and is commonly linked to syndactyly (Umair *et al.,* 2018).

1.1 Preaxial Polydactyly

Preaxial polydactyly (PPD) refers to an extra digit adjacent to the first digit on a radial side of the hand (thumb) or on a tibial side of the foot (toe). Following PAP, it ranks among the most prevalent congenital hand abnormalities, having a probability of 0.08-1.4/1000 in live births (Manske *et al.,* 2018). PPD is further divided into 4 types as shown in table 1.1.

1.1.1 Preaxial Polydactyly Type 1

PPD type 1 (OMIM 174400) also referred to as 'thumb polydactyly', represents a duplication of the bi-phalangeal thumb. It is usually inherited in a unilateral form whereas in a bilateral form, upper limbs are more affected than lower ones and right-hand PPD is more prevalent than left-hand PPD. Type 1 PPD is one of the most common polydactyly compared to other types (Malik *et al.,* 2014). Study shows that preaxial polydactyly type-1 is caused by the *GLI1,* mapped on chromosome 12q13.3 and is inherited in an autosomal recessive form (Ullah *et al.,* 2019).

1.1.2 Preaxial Polydactyly Type 2

PPD type 2/ tri-phalangeal thumb (TPT) polydactyly (OMIM 174500) is different from PPD-1, as it has three phalanges in the extra thumb digit with disproportionately thin and long 1st metacarpal and epiphysis on both ends. PPD type 2 is often bilateral and symmetrical having an autosomal dominant and incomplete penetrance (Umair *et al.,* 2018). TPT is reported to be caused by ZRS of *LMPR1* gene within its intron 5, which is located on chromosomal region 7q36.3 (Lettice *et al.,* 2003).

1.1.3 Preaxial Polydactyly Type 3

PPD type 3 (OMIM 174600) is also known as an index finger polydactyly in which an index finger is usually duplicated. It differs from PPD-2 as the thumb in type 3 is replaced with one or two triphalangeal digits and the metacarpal shows a distal epiphysis. It often shows autosomal dominant segregation. The unknown gene is responsible for PPD type 3 (Kyriazis *et al.,* 2023).

1.1.4 Preaxial Polydactyly Type 4

PPD type 4 (OMIM 174700) is also known as polysyndactyly of the hand. In PPD-4 thumb is duplicated mildly and third and fourth fingers of hand or toes are affected by syndactyly in an autosomal dominant fashion. The *GLI3* gene on chromosomal locus 7p14.1 is known to cause PPD type 4 (Kyriaziz *et al.,* 2023).

Table 1.1: PPD Classification.

Phenotype	OMIM ID	Locus	Genes	Inheritance
PPD1	165220	12q13.3	*GLI1*	AR
PPD2	174500	7q36.3	*LMPR1*	AD
PPD3	174600	U	*U*	AD
PPD4	174200	7p14.1	*GLI3*	AD

U: unknown, AD: autosomal dominant, AR: autosomal recessive

1.2 Mesoaxial Polydactyly

Mesoaxial polydactyly/central polydactyly is a relatively rare kind of polydactyly, accounting for just 5-15% of all other polydactylies. It affects mid digits of the hands or foot and is the hidden duplication as tissue mass is present in the center of the hand

as synonychia or with apparent syndactyly. It is further classified into three subtypes (Bubshait and Dalal, 2022):

1.2.1 Type I Duplications

Duplications of type I lack an osseous or ligamentous link to the neighboring digit.

1.2.2 Type II Duplications

Duplications of type II have ligamentous and soft tissue features inside the duplicitous digit and share a phalanx, bifid meta-carpal, or a joint with the neighboring digit. It may have simultaneous syndactyly or no syndactyly.

1.2.3 Type III Duplications

Duplication of type III have a completely formed metacarpal.
Umair et al., (2018) reported that in central polydactyly fourth digit is most frequently duplicated and the deformity is typically bilateral with the dominant inheritance pattern.

1.3 Postaxial Polydactyly

Postaxial polydactyly (PAP) (OMIM 174200) refers to one or more additional digits at the ulnar/fibular side of the hand/foot respectively. It is about 75-87% more frequent than other polydactylies. PAP prevalence varies slightly depending on ethnic background, at 1-2/1000 live births. PAP may be either unilateral or bilateral. Several congenital anomalies are associated with cases of bilateral PAP in limbs of the lower and upper extremities. PAP is subdivided into two categories depending on the duplicated extra digit(s); Postaxial Type A (PAP-A), and Postaxial Type B (PAP-B). Both types differ in their prevalence, inheritance pattern, and severity (Verma and El-Harouni, 2015).

1.3.1 Postaxial Polydactyly Type A

In postaxial polydactyly type-A (PAP-A), a completely formed additional digit (with bone) grows at the $5^{th}/6^{th}$ metacarpal. The duplicated digit contains one to three bony elements and a fully developed nail on it. As the extra digit is non-functional, it may pose complications in normal life activities. Type-A is inherited in either an

autosomally dominant or an autosomally recessive way. In literature, PAP-A is further classified into 11 subtypes (PAP-A1 to PAP-A11) (as shown in table 1.2) on the basis of genetics (Umair *et al.,* 2018).

1.3.1.1 Postaxial Polydactyly Type A-1

Postaxial Polydactyly A type 1 (OMIM 174200) is the most widespread digit anomaly, resulting due to heterozygous mutants in the *GLI3* (OMIM 165240), mapped on 7p14.1 chromosomal position. In non-syndromic conditions, extra digit grows completely on one side of 5th metacarpal, inherited autosomally dominantly. *GLI3* belongs to the *GLI* family that encodes transcription factor, C2H2, involved in the SHH limb bud development pathway, particularly in an anteroposterior axis. There are numerous skeletal abnormalities linked to 330 reported variants in the *GLI3* gene, in which PAP-A is the 3rd dominant condition, the other two are Pallister-Hall Syndrome (PHS) (OMIM 146510), Greig Cephalo-polysyndactyly Syndrome (GCPS) (OMIM 175700) (Radhakrishna *et al.,* 1997).

1.3.1.2 Postaxial Polydactyly Type A-2

Postaxial Polydactyly A type 2 (OMIM 602085) is inherited in either unilateral or bilateral isolated form with clinical features overlapping with PAP-A1. The causative gene is not discovered yet (Ahmad *et al.,* 2023), but located on 13q21-q32 chromosome (Akarsu *et al*., 1997).

1.3.1.3 Postaxial Polydactyly Type A-3

Postaxial Polydactyly A type 3 (OMIM 607324) was discovered for the first time in a Chinese family in a dominant form with characteristics of PAP type A as well as B. The affected members of the family exhibited fully developed and functional bilateral PAP but had different expression patterns (Zhao *et al.,* 2002). The causative gene for PAP-A3 is still unknown, but caused by mutation at chromosomal location 19p13.2-p13.1.

1.3.1.4 Postaxial Polydactyly Type A-4

Postaxial Polydactyly A type 4 (OMIM 608562), mapped on chromosome 7q22, was determined in a large Dutch family. PAP-A4 exhibits an autosomal dominant

inheritance pattern. PAP-A4 is characterized by PAP and in some cases, with partially cutaneous syndactyly. The expression of polydactyly and syndactyly is variable in PAP-A4, suggesting that these phenotypes have substantial penetrance and genetic heterogeneity (Galjaard *et al.,* 2003). The responsible gene is still unknown.

1.3.1.5 Postaxial Polydactyly Type A-5

Postaxial Polydactyly A type 5 (OMIM 263450) was traced on chromosome 13q13.3-q21 initially in the consanguineous family from the Sindh province of Pakistan. The affected individuals exhibited bilateral PAP in both the lower and upper extremities, hallux deformity, cutaneous syndactyly in some members, and feet with a 5th metatarsal that resembles a fork. PAP was inherited in the family in an autosomal recessive pattern. Ten candidate genes were sequenced in the present study but the responsible variant for the autosomal recessive PAP-A was not identified on the present locus (E-Kalsoom *et al.,* 2012).

1.3.1.6 Postaxial Polydactyly Type A-6

Postaxial polydactyly A type 6 (OMIM 615226) was initially mapped on chromosome 4p16.3 in the closely related Pakistani family. It was reported as a second locus for PAP-A with an autosomal recessive inheritance mode. The affected individuals had a bilateral, completely developed 5th finger in their hands as well as in their feet with either radial or ulnar deviation in different members and, in some cases, have a duplicated distal phalanx. No other additional symptoms were observed in affected family members which indicated isolated PAP. The WES of the affected family discovered a missense homozygous mutation in *ZNF141* (OMIM 615226) gene (Kalsoom *et al.,* 2013).

1.3.1.7 Postaxial Polydactyly Type A-7

Postaxial Polydactyly A type 7 (OMIM 617642) is an autosomal recessive disorder, resulting due to a mutation in an *IQCE* gene, mapped on chromosomal position 7p22.3. PAP-A7 was initially found in a closely related Pakistani family with isolated bilateral PAP restricted only to feet (Umair *et al.,* 2017). *IQCE* gene encodes a ciliary protein present in the primary cilia base, that participates in the Hedgehog pathway (Estrada-Cuzcano *et al.,* 2020).

1.3.1.8 Postaxial Polydactyly Type A-8

Postaxial polydactyly A type 8 (OMIM 618123) is an autosomal recessive condition, resulting due to a mutation in *GLI1* (OMIM 165220) gene, on chromosomal position 12q13.3 (Palencia-Campos *et al.,* 2017). Clinical phenotypes of this type of polydactyly includes bilateral PAP in lower/upper limb extremities, shorter lower limbs, nail dysplasia, and an atrial septal defect.

1.3.1.9 Postaxial Polydactyly Type A-9

Postaxial polydactyly A type 9 (OMIM 618219) is characterized by an isolated PAP in both the upper as well as lower limb extremities. It has an autosomally recessive pattern with a mutation in *FAM92A* (OMIM 617273) gene located on chromosome 8q22.1. PAP-A9 was initially identified in a consanguineous Pakistani household with three reported brothers displaying isolated PAP. Radiographs of the hand and feet of one affected member showed a sixth digit attached to the 5th metacarpal of both hands and an extra digit of feet was attached without the metatarsal (Schrauwen *et al.,* 2018).

1.3.1.10 Postaxial Polydactyly Type A-10

Postaxial Polydactyly A type 10 (OMIM 618498) was found in two parentally linked Pakistani families, exhibiting bilateral polydactyly in hands as well as feet with varying metatarsal size and clinodactyly in some members. It is inherited as autosomal recessive condition, caused by mutation in *KIAA0825* (OMIM 617226) gene located on chromosome 5q15 (Ullah *et al.,* 2019).

1.3.1.11 Postaxial Polydactyly Type A-11

Postaxial Polydactyly A type 11 was identified in a single Pakistani family affected by bilateral non-syndromic PAP with mild syndactyly in the 2nd as well as 3rd toes. It is inherited in autosomal recessive form and caused by mutation in *DACH1* gene (Umair *et al.,* 2021) located on chromosome 13q21.33. No results of this type of PAP are reported on OMIM.

Table 1.2: PAP Classification

Phenotype	OMIM ID	Locus	Genes	Inheritance
PAP1	174200	7p14.1	*GLI3*	AD, AR
PAP2	602085	13q21-q32	*U*	AD
PAP3	607324	19p13.1-p13.2	*U*	AD
PAP4	608562	7q22	*U*	AD
PAP5	263450	13q13.3-q21	*U*	AR
PAP6	615226	4p16.3	*ZNF141*	AR
PAP7	617642	7p22.3	*IQCE*	AR
PAP8	618123	12q13.3	*GLI1*	AR
PAP9	618219	8q22.1	*FAM92A*	AR
PAP10	618498	5q15	*KIAA0825*	AR
PAP11	U	13q21.33	*DACH1*	AR

U: unknown, AD: autosomal dominant, AR: autosomal recessive

1.3.2 Postaxial Polydactyly Type B

A vestigial 6th finger is present in PAP-B affected individuals, at the base of the phalanx and metacarpal/metatarsal of hand/feet respectively. This additional finger is also known as "pedunculated postminimi". The additional finger is much smaller than the 5th finger and is present as a sac of tissue with a single phalanx and no bone and nail, which can be easily removed by surgery (Holmes *et al.,* 2018).

2 Syndromic Polydactyly

221 syndromic polydactylies and 120 syndromic oligodactyly disorders are been reported by the London Dysmorphology database (Ahmad *et al.,* 2023). '8659' entries appear on typing the word 'Syndromic Polydactyly' in the online OMIM database (https://www.omim.org/). The most reported digit abnormalities are Ellis-Van Crevald Syndrome (OMIM 225500), Pallister-Hall Syndrome (OMIM 146510), Bardet-Biedl Syndrome (OMIM 617119), and Greig Cephalopolysyndactyly Syndrome (OMIM 175700) and many more (Ahmad *et al.,* 2023).

Aims and Objectives

The current study aim is to identify genetic variants in two Pakistani families of Postaxial polydactyly phenotype. This study also aims to develop a genotype and phenotype correlation among affected families. To achieve this objective, Whole Exome Sequencing (WES) of family members was performed, and possible candidate genes were shortlisted using different bioinformatics tools and software, followed by conventional Sanger DNA Sequencing for confirming its segregation in the family. Using various online bioinformatics tools, the impact of the pathogenic variants was detected. This investigation holds the potential to contribute to the accurate diagnosis of genetic skeletal disorders and play a crucial role in providing genetic counseling to the affected families.

Chapter 2
MATERIALS & METHODS

MATERIALS AND METHODS

Research Approval

Two Pakistani Postaxial polydactyly (PAP) families were included in the current research study. The Institutional Review Board (IRB) of Quaid-i-Azam University Islamabad, Pakistan approved the present work. Affected family members or elders of the influencing family members provided written signed consents for genetic investigations.

Clinical Evaluation and Families Recruitment

A field survey of two families with Postaxial polydactyly phenotypes was conceded in the Khyber Pakhtunkhwa (KP) province of Pakistan. The research, potential outcomes, and perspective for the future were explained to the families who agreed to take part in the study. The recruited families were affected with Non-Syndromic PAP showing an Autosomal Dominant (AD) and an Autosomal Recessive (AR) inheritance pattern. Photographs and detailed medical records of affected family members were taken.

Pedigree Construction

After interviewing well-informed family members, pedigrees were designed using the proposed concept by Bennett *et al.,* 2008. Hollow circles and squares were used to denote unaffected females and males respectively whereas those with dark shading represented afflicted members. The crossline over the symbols represented deceased members. In pedigree, double horizontal lines indicate consanguineous marriage while vertical lines were used to indicate generation. Each consecutive generation was represented by a Roman number from top to bottom, and its members were identified by Arabic numerals.

Blood Sample Collection

Using hypodermic syringes, venous blood (3-5 ml) samples were taken from both affected and unaffected available family members. As soon as blood was collected, it was quickly transferred to a container containing EDTA [BD; 10ml vacutainer, K3-EDTA, Franklin Lakes NJ, USA] to prevent a blood clot. Until DNA extraction, the obtained blood samples were kept at 4ºC.

Genomic DNA Extraction

The blood samples were incubated for about an hour at room temperature after being previously stored at 4°C. The DNA was isolated from whole blood by the manual Phenol-chloroform method or by a commercially accessible kit.

a**) Phenol-Chloroform Method**

- On day 1, prepared an Eppendorf with 700µl of blood and 700µl of solution-A, shake it 6-7 times, and let it sit at room temperature for 30 to 35 minutes.
- An Eppendorf was centrifuged at 13,000 rpm for 1min.
- The supernatant was removed, and the leftover pellet was then reinserted in 500µl of solution-A, and centrifuged at a speed of 13,000 rpm for 1min.
- After discarding the unwanted supernatant, the remaining pellet was incubated overnight at 37°C with 450µl of solution B, 17µl of 20% SDS, and 13µl of proteinase K.
- On day 2, the Eppendorf containing the dissolved pellet was mixed with an equal volume (each 250µl) of Solution-C and Solution-D.
- After that tubes were centrifuged at a speed of 13,000rpm for 10 min. to form three distinctly distinguishable layers.
- Using a new Eppendorf, the topmost aqueous layer was proficiently transferred, mixed with 500µl of Solution-D, and centrifuged once more for 10 min at 13,000rpm.
- The DNA-containing aqueous layer was collected in an autoclaved Eppendorf tube with 55µl sodium acetate and 450µl chilled isopropanol to precipitate out the DNA.
- To concentrate the DNA at the bottom of the tube, Eppendorf was centrifuged for 10 minutes at 13,000rpm. The supernatant was discarded and the DNA pellet was again centrifuged at 13,000rpm for 7 minutes after being rinsed with 200µl of 70% ethanol.
- After centrifugation, any remaining ethanol was taken out and the pellet was dried using an Eppendorf vacuum concentrator “5301” [Hamburg, Germany] for 15-25 minutes at 45°C.

- The dried-out DNA pellet was diluted in 120-200µl of Tris-EDTA (TE-Buffer) and stored at 4°C.
- Composition of the solutions used for DNA Extraction is shown in table 2.1.

Table 2. 1: Composition of the solutions used for DNA Extraction

Solutions	Compositions
Solution A	Sucrose (0.32) + MgCl2 (5mM) + Tris. (10mM: pH 7.5) + 1% (v/v) Triton-X-100/
Solution B	EDTA (2mM:pH8.8) + NaCl (400mM) + Tris (10mM: pH7.5)
Solution C	Phenol
Solution D	Chloroform + Isoamyl Alcohol (24:1)
20% SDS	10g in 50 ml water.
70% Ethanol	70 ml ethanol in 30 ml distilled water.

b) Extraction of DNA through the Kit Method

A commercial kit from Sigma-Aldrich, Gene Elute Blood Genomic DNA kit, was used to extract genomic DNA from blood.

- In a 1.5ml Eppendorf tube, 200µl of a whole blood sample, 200µl of lysis buffer, and 20µl of PK enzyme were homogenized together and were placed in a water-based bath to incubate around 55°C for 10 min.
- 200µl of 100% ethanol had been added, and the mixture was vortexed for 15-20 seconds.
- The entire combination was poured into the mini-prep column and centrifuged for one min at 8000 rpm.
- The flow-through was eliminated, and the DNA was then washed with 500µl of each wash buffer (WB1 & WB2) and centrifuged for 1-3 minutes at 8,000-13,000 rpm respectively.
- To remove the remaining washing buffers, an empty spin was performed at 13,000 rpm for 1 min.
- After washing, 250µl Elution Buffer was added and underwent incubation at 25°C for 10-15 minutes.

- Then, utilizing a high-speed centrifuge, DNA was extracted, placed in a tube, and stored at 4°C.

Agarose Gel Electrophoresis (1%)

1% agarose gel was used to check the DNA's quality. To generate a total volume of 100ml, 90ml of distilled water was mixed with 10ml Tris-Borate EDTA (TBE) also called 10X buffer solution. The solution was poured into a beaker and 1g of agarose powder was added after weighing. The DNA was then stained by adding 6 ml of ethidium bromide (EtBr) dye to the solution. The gel was transferred into a gel casting tray, where it was left to solidify for roughly 30 minutes. Afterwards, the gel was poured into an electrophoresis tank with 1X running buffer. DNA samples (3µl) were put into a gel along with an equivalent amount of loading dye (bromophenol blue) and the voltage was adjusted to 120 volts. The DNA strands were visualized using a UV trans-illuminator [Biometra, Gottingen, Germany].

DNA Quantification and Dilution

The Colibri micro-volume spectrophotometer (Titertek Berthold, Germany) was used for the quantitative analysis of DNA and the readings were obtained at an optical density (OD) of 260 nm. First, the spectrophotometer was blanked and measured by using 2µl of TE buffer and then 2µl of DNA samples were loaded to measure their concentration in ng/µl units. Depending on DNA concentration, DNA was diluted to 20-30 ng/µl by adding PCR water.

Whole Exome Sequencing

WES was conducted at the Yale Centre for Genome Analysis (YCGA), which was subsidized by the Higher Education Commission (HEC) of Pakistan, the Yale Paediatric Genome Discovery Programme (PGDP), the Yale School of Medicine in Connecticut, USA, and the Center of Inherited Diseases at Taibah University Madinah, SA.

Sample DNA (3-5µg) of whole members of the first family and a single member of the second family was provided for WES to YCGA. IDT-xGen Capture kit from the USA was used to prepare the sequencing library, and the Illumina (HiSeq4000) platform carried out the WES. Paired-end sequence readings were transferred to

FASTQ format and compared to the UCSC reference human genome (hg19). The Genome Analysis Tool kit (GATK.v3.4) was used for Variants (CNV, SNV) detection, variant calling, indel realignment, removal of duplications, and Quality recalibrations (Van-der-Auwera *et al.,* 2013) and AnnoVar was used for Annotation. A mean depth of 80-120 independent reads per targeted base was used to sequence the members. On average, 93.7-94.8% of all the samples had more than eight independent reads, indicating high confidence in all the exome variants. Variants with depth score (QD≥2) and high-quality sequencing reads with at least 10 total reads were filtered. Variants were then selected based on their nature (frame-shift mutant, splice-site variant, missense variant), function and expression. The following criteria were set for shortlisting candidate genes with Allele frequency <0.0001, CADD Phred score >13, and nature of inheritance pattern (autosomal dominant or recessive).

Variants were chosen after analyzing them on various databases:

- gnomAD (https://gnomad.broadinstitute.org/)
- Mutation Taster (https://www.mutationtaster.org/)
- VarSome (https://varsome.com/)
- ClinVar (https://www.ncbi.nlm.nih.gov/clinvar/)
- HGMD (https://www.hgmd.cf.ac.uk/)
- DynaMutt (https://biosig.lab.uq.edu.au/dynamut2)

Further segregation of the variants in all family members was confirmed by Sanger Sequencing.

Primer Designing

To examine the segregation of pathogenic variants, identified through WES in PAP families, primers were designed using various online bioinformatics tools which include 'Primer 3 Web' https://primer3.ut.ee/, 'Primer Stats' https://www.bioinformatics.org/sms2/pcr_primer_stats.html and 'UCSC In-Silico PCR' https://genome.ucsc.edu/cgi-bin/hgPcr. The self-annealing, GC content, and primer dimerization were optimized during primer annealing. The designed amplified primers were then checked on 1% agarose gel. Designed primers are shown in table 2.3.

PCR Amplification

The targeted genes were amplified through primers with the Polymerase Chain Reaction (PCR) by making a total volume of 25µl. The PCR tests were performed using a T3 Thermocycler (Biometra, Germany). Following chemicals were used in the mentioned concentrations to perform the PCR: Template DNA 1µl, dNTPs 0.5µl, reverse primer 1µl, forward primer 1µl, MgCl2 2µl, Taq Polymerase 0.5µl, PCR Buffer 2.5µl, and 16.5µl of PCR water to make a total volume of 25µl. 1.5µl of DMSO was also added to GC-rich genes. The following conditions were set on the PCR as shown in table 2.2.

Table 2.2 PCR conditions

PCR Stage	Temperature	Time Duration	Cycles
Initial Denaturation	94-96°C	7 minutes	30-35
Final Denaturation	94-94°C	35 seconds	
Primer Annealing	56-64°C	30 seconds	
Initial Extension	72°C	35 seconds	
Final Extension	72°C	10 minutes	
Hold	4-10°C	Pause	

Agarose Gel (2%)

Products of the above PCR were analyzed on 2% agarose gel. 2g of agarose was added into 10 ml of 10X TBE and 90 ml of distilled water to prepare a 100 ml gel. The mixture was microwaved for about 2 minutes to dissolve the added ingredients. Then 6µl of Et.Br. was added to the mixture and poured into a gel tray to let it solidify for about 30 minutes. After solidification, the gel was transferred to a gel tank and 3µl PCR amplified products were loaded along with 3µl of bromophenol blue dye. Electrophoresis was performed at 90 volts for about 45 minutes and bands were visualised by a gel doc UV analyzer.

Purification Protocol

The amplified PCR product was purified by using Axygen Biosciences PCR clean-up Kit (Invitrogen) through the following steps:

- The amplified product was combined thoroughly with around 75µl of Binding buffer. The mixture was then put into a column with a 2ml collecting tube and

centrifuged at 13,000 rpm for about 1 min. The filtrate accumulated in the collection tube was taken out.

- The column was double-washed using 450µl and 350µl of washing buffer, each time centrifuged at 13,000 rpm for about 1 min. The liquid was discarded after being centrifuged.
- After discarding, a 2-minute empty spin was performed on the purification column to remove contaminants and impurities.
- The column was then placed in an Eppendorf tube and 25µl of elution buffer was added after placing it in an incubator at 33°C for 10 minutes.
- The purified DNA was obtained by centrifuging the purification column and Eppendorf for 10 min. at 13,000 rpm. This purified DNA was then analyzed on 2% agarose gel.

Sanger Sequencing Analysis

The purified DNA of specific base pair size was then subjected to commercially available Sanger Sequencing and results were analyzed through the Bio-Edit Alignment software tool (https://bioedit.software.informer.com/7.2/). Chromatograms of affected and normal members were then analyzed with the reference sequence of genes obtained through the UCSC genome browser.

Table2. 3 List of primers used for Segregation Analysis

Sr.No.	Gene	Primers Sequence	Product Size
1	FGFR3(F)	GATGCCACTGACAAGGACCT	466
	FGFR3(R)	CTGAAGCCTCTCCACCTCTC	
2	WNT10A(F)	TTCCTTGTGCCAGACTCTCC	295
	WNT10A(R)	AGTGCATCCAGTTGTAAGCG	
3	TMPPE(F)	GGAGAGGTCACCCACAATCA	286
	TMPPE(R)	GGGCAGCCTTGAGAAGACAA	
4	CZIB(F)	GCATCTTAGGCCTGACTCCA	260
	CZIB(R)	CCTTTCTGGGTCTTGGTCTC	
5	SMO(F)	TGGAAAGAATGGCATCGCT	334
	SMO(R)	GCACACAGATTATTTGGAAG	
6	CFAP57(F)	TCCACCAGTCAGTTCTCCAC	221
	CFAP57(R)	TGCTGCTGGGGAACAAATG	

Chapter 3
RESULTS

RESULTS

In this chapter, we described the clinical and genetic findings of Family A and Family B segregating non-syndromic postaxial polydactyly in an autosomal dominant and recessive inheritance pattern respectively. The WES followed by Sanger sequencing was performed to identify potential disease-causing variants in affected members of both families.

Family A

Family A belongs to District Lakki Marwat, Khyber Pakhtunkhuwa province of Pakistan. Pedigree shows a total of four members, which includes two affected members (III-2 and IV-1) and two carrier normal members (III-1 and IV-2), that participated in the current study (Fig.3.1).

Clinical Features

Both affected members (III-2 and IV-1) of family A perceived unilateral postaxial polydactyly type A in an autosomal dominant inheritance pattern. The upper limbs of both members remained unaffected, while PAP-A was restricted to the lower limbs only. Syndactyly and brachydactyly at the 4^{th} and 5^{th} toes were observed (Fig.3.2). Additionally, Hallux valgus was seen in one affected member (III-2). Both of the members did not exhibit any other abnormality, suggesting isolated PAP.

Genetic Investigation

DNA of both affected members of family A were subjected to Whole Exome Sequencing. Analysis of the exome data filtered 51,612 variants. To find disease-causing variants in the Excel file, various filters were applied. Focus was to only search for pathogenic missense, non-synonymous, frame-shift and non-sense deletions/insertions. At first, only splice-site and exonic variants were selected for the heterozygous genotype. In the second filter, the CADD Phred score of ≥ 13, allele frequency ≤ 0.005 was selected. Two variants in two genes were shortlisted for the segregation analysis which includes *WNT10A* [Exon3: c.383G>A] and *FGFR3* [Exon13: c.1657G>A]. A missense variant [c.1657G>A: p. Val555Met] in exon 13 in the *FGFR3* gene, located on chromosome 4 was present. The heterozygous variant in

the *FGFR3* gene was segregated through Sanger Sequencing in an affected family (Fig.3.5). The variant [c.1657G>A] had a CADD Phred score of 27.3. The ***FGFR3*** variant was identified as a **novel** in PAP and was absent in ExAC, HGMD, 1000G, and GnomAD. Also, the *FGFR3* gene [Exon13: c.1657G>A] will be reported for the first time in a non-syndromic PAP. While the Sanger sequencing of *WNT10A* showed no segregation in a family.

Homology modeling of wild-type and mutated *FGFR3* predicted a stability change of -0.7 kcal/mol. Wild-type Val555 makes a hydrogen bond with Ala506 as shown with red dashes (Fig.3.7-A) while the mutant Met555 makes extra hydrogen bonds with Val505, Leu542, and Met529 along with Ala506, as shown with red dashes (Fig.3.7-B). These additional hydrogen bonds are likely to disrupt the protein folding and its interaction with other molecules, which changes the function of *FGFR3.*

Family B

Family B was sampled from Nawabshah, Sindh province of Pakistan, for the clinical and genetic analysis of the Polydactyly. The pedigree showed three affected members; i.e. one female (IV-2) and two males (IV-1 and III-3) (Fig.3.3). Affected member III-3 was died of natural death before sampling.

Clinical Features

The affected member (IV-1) exhibited bilateral postaxial polydactyly type A in the upper limbs and syndactyly and brachydactyly in the 5^{th}-7^{th} fingers of the left hand. The affected individual also showed clinodactyly of 5^{th} finger in right hand. Polydactyly in both hands were articulated from the base of 5^{th} finger (Fig.3.4). According to family members, the affected deceased member (III-3) had exclusively bilateral postaxial polydactyly in hands. Member (IV-2), who did not consent to provide clinical photographs, manifested bilateral postaxial polydactyly in hands and feet. Affected members were mentally normal. Upon physical examination, no other associated symptoms were found in the affected family, indicating isolated polydactyly.

Genetic Investigation

The DNA of affected member (IV-1) was subjected to Whole Exome Sequencing. 30,853 variants were filtered through exome analysis. Various filters were applied to search potential pathogenic variants. The intronic, non-coding, intragenic, and low-quality variants were filtered out first. Based on the pedigree, only homozygous variants were selected. The CADD Phred score of ≥ 13, splice site (+/- 12bp), and allele frequency ≤ 0.005 were selected. Five variants of different genes were shortlisted as candidate genes for segregation analysis. This included *SMO, CFAP57, Rab25, CZIB,* and *TMPPE*. All the genes variants were considered novel for causing postaxial polydactyly. *Rab25* [Exon2: c.223C>T] showed no segregation by Sanger sequencing in affected family. While *SMO* [Exon10: c.1792G>A], *CFAP57* [Exon5: c.921T>G], *CZIB* [Exon4: c.172C>T], and *TMPPE* [Exon2: c.595C>T] were successfully segregated in family. *CFAP57, CZIB,* and *TMPPE* are not previously linked to polydactyly while *SMO* has been previously reported to cause postaxial polydactyly. Based on literature review, ***SMO*** was selected as a causative gene with a **novel variant** [c.1792 G>A; p. Gly598Arg] responsible for disease phenotype in affected family (Fig.3.6). The variant had a CADD Phred score of 25.4 and was identified as a missense variant located on chromosome 7q32.1. This variant was reported pathogenic by Mutation_Taster, Varsome, PolyPhen, and HGMD and was absent in ExAC, HGMD, GnomAD, All of Us and Bravo, suggesting the variant to be normal.

The stability difference predicted by Homology Modeling of wild-type and mutated *SMO* was -0.56 kcal/mol. Wild-type Gly598 makes Hydrogen bonds with His596 and Ala601 (Fig.3.8-A). While mutant Arg598 makes an extra Hydrogen bond with Ser595, shown with red dashes (in Fig. 3.8-B). It is highly probable that extra hydrogen bonds can hinder the correct folding of proteins and their ability to interact with other molecules, ultimately leading to a change in the functions of *SMO.*

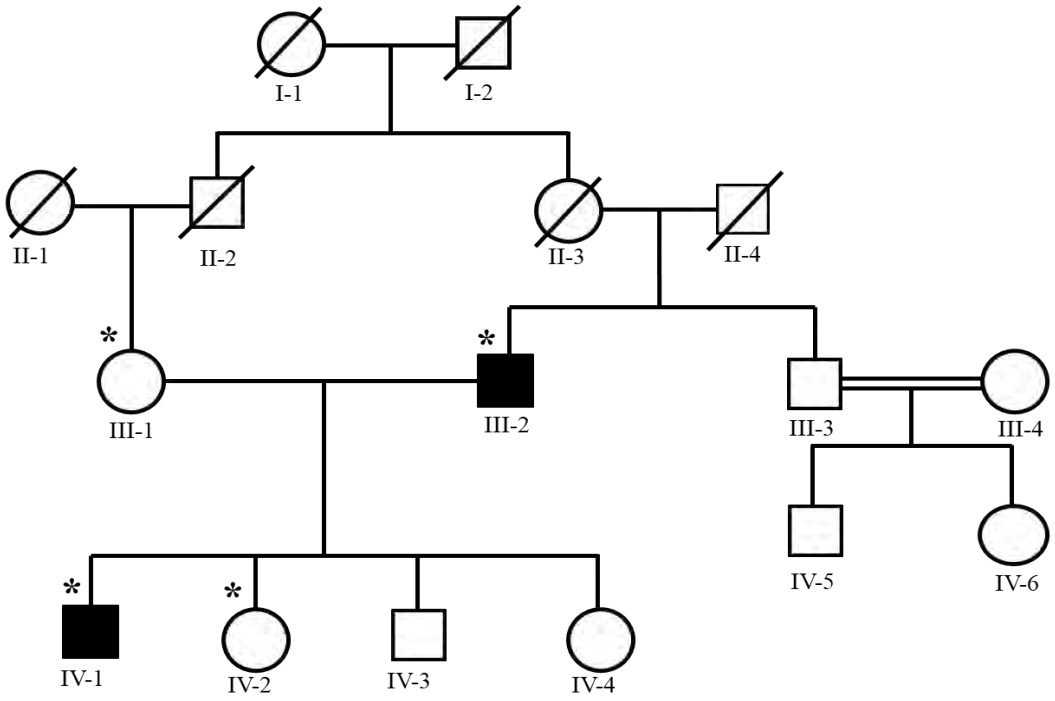

Figure 3.1: Pedigree of Family A, shows an autosomal dominant inheritance pattern. Squares are used to show males, while circles indicate females. Black-filled shapes designate affected members whereas colorless shapes represent normal members. An asterisk (*) sign indicates sampled members. The double line between male and female indicates consanguinity. The crossline above the sample represents a deceased member. The generation position and family member's lineage are shown by Roman and Arabic numerals.

Figure 3.2: Clinical features of an affected member [III-2] of Family A, expressing postaxial polydactyly along with syndactyly and brachydactyly of 4^{th}-6^{th} right feet. The condition known as Hallux Valgus was found in both feet.

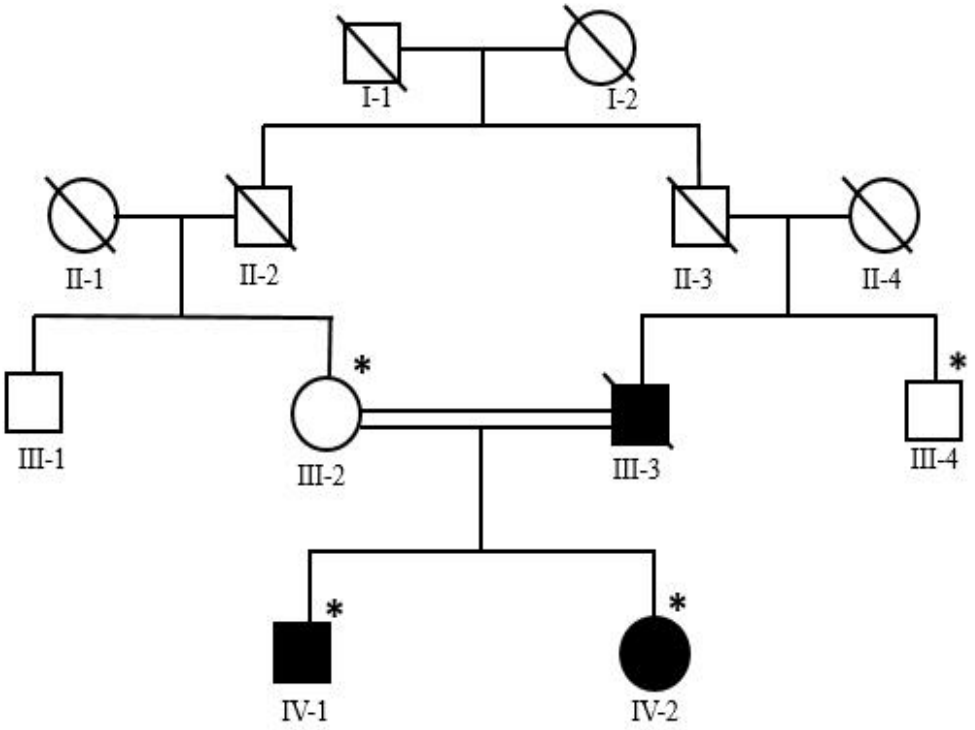

Figure 3.3: Family B Pedigree shows an autosomal recessive inheritance pattern. Females are represented by a circle, whereas males are shown by squares. Black-colored squares and circle denote affected members while a colorless symbol represents unaffected members. A cross line indicates deceased members and the consanguineous union is shown by double lines. An asterisk (*) sign indicates members whose blood was drawn. Roman numerals are used to express generation numbers while Arabic numerals are used to indicate to indicate a family member's position within a generation.

Figure 3.4: Clinical features of an affected member [IV-1] of family B, expressing bilateral postaxial polydactyly in hands as well as syndactyly and brachydactyly in the 5^{th}-7^{th} fingers of the left hand. The affected member also showed clinodactyly of the 5^{th} finger in the right hand.

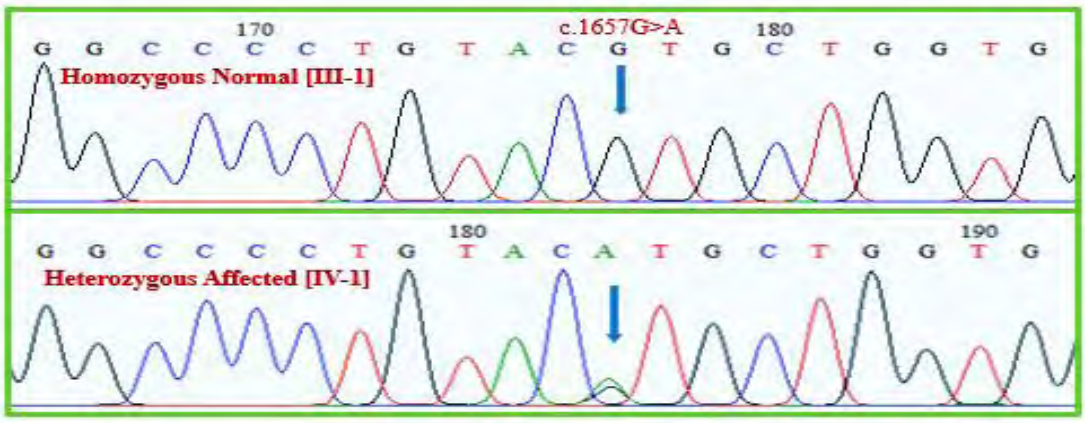

Figure 3.5: Sanger Sequencing chromatograms and segregation is shown in family A. Homozygous normal (upper panel) and heterozygous affected (below panel) are shown. The blue arrow represents missense mutation [c.1657G>A] in the *FGFR3* gene.

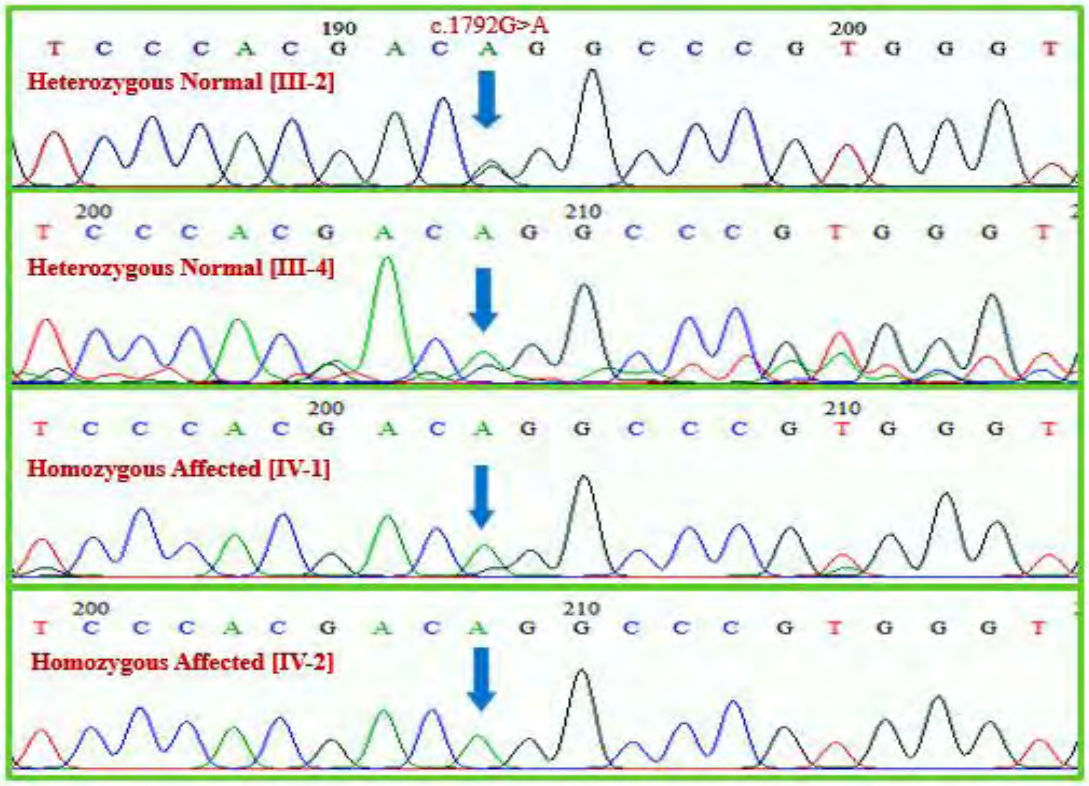

Figure 3.6: Sanger sequencing chromatograms are shown of family B. Heterozygous normal (above two) and homozygous affected (below two) expressing missense mutation [c.1792G>A] identified in the *SMO* gene.

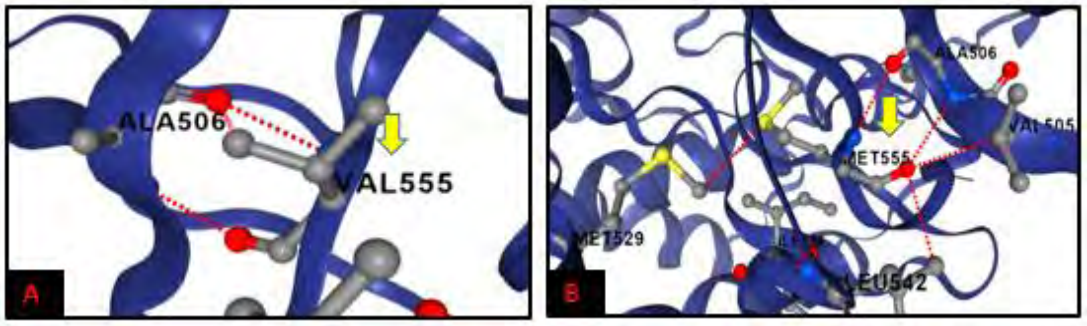

Figure 3.7: Homology Modeling of wild-type and mutated *FGFR* protein. (A) In wild-type, at position 555 Valine making a hydrogen bond with Alanine which is at position 506, shown with red dashes. (B) While in mutated protein, at position 555 Methionine (reference amino acid: VAL) making additional hydrogen bonds with Valine, Leucine, and Methionine at positions 505, 542, and 529 respectively. (https://biosig.lab.uq.edu.au/dynamut2)

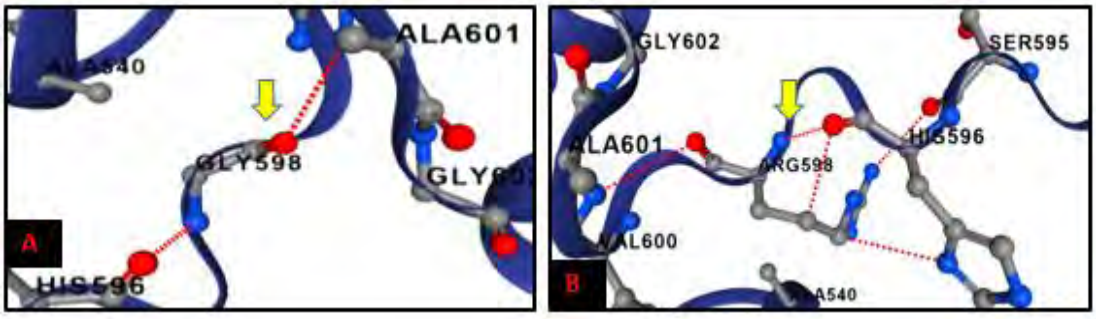

Figure 3.8: Homology Modeling of wild-type and mutated *SMO* protein. (A) In wild-type SMO, Glycine at position 598 makes a hydrogen bond with Alanine and Histidine at positions 601 and 596 respectively, shown with red dashes. (B) While in mutated SMO, Arginine at position 598 (reference amino acid: GLY) makes an extra hydrogen bond at position 595 with Serine. (https://biosig.lab.uq.edu.au/dynamut2)

Table 3.1: Analysis of variants detected in exome data in PAP families

Family ID	**A**	**B**
Gene	***FGFR3***	***SMO***
Nature of Mutation	Missense mutation	Missense mutation
Mutation Detail	NM_001163213 exon13:c.G1657A p.Val555Met	NM_005631 Exon10:c.G1792A p.Gly598Arg
Status of Mutation	Novel Variant	Novel Variant
No. of Homozygotes	0	0
Allele Frequency	0.000176	0.00002468
CADD Score	27.3	25.4
Mutation Taster	Pathogenic	Pathogenic
PolyPhen Score	Probably Damaging (0.962)	Probably Damaging (0.999)
SIFT	Deleterious (0.01)	Tolerated (0.05)
Varsome	Likely Pathogenic	Uncertain significance

Chapter 4
DISCUSSIONS

DISCUSSION

The skeletal system serves several essential functions that include providing support for the body, protecting organs, facilitating linear growth, enabling mobility, and acting as a storage reservoir for minerals and blood cells. (Krakow and Rimoin, 2010). Skeleton patterning and bone development are tightly regulated processes in the presence of several transcription factors and bone signaling pathways. Any mutation in these pathways or factors that disturbs the skeletal developmental process leads to Genetic Skeletal Dysplasia (GSD). In the Pakistani population, several of these disorders segregating in autosomal dominant, recessive, and X-linked patterns have been characterized, both in non-syndromic and syndromic forms. 82.5% of parents in diverse regions of Pakistan are blood-related due to social, economic, religious, and cultural factors. All four of Pakistan's provinces have GSD cases on record. In Pakistan, there is a significant lack of attention given to rare genetic disorders such as GSDs. This issue is exacerbated by the country's ongoing challenges in providing sufficient genetic testing services. These conditions affect a small portion of the population, yet they can have a enormous impact on the lives of those who are affected. More resources must be devoted to addressing this issue and providing support to those who need it (Umair *et al.,* 2019).

Polydactyly, a genetic condition also known as 'Hexadactyly', is characterized by the presence of additional digits on the hands or feet. This condition is inherited and can occur in varying degrees, ranging from a small skin tag to a fully-formed extra finger or toe with bone, muscle, and nail. While it may not necessarily cause functional impairment, it can sometimes affect the normal development and movement of the affected limb. Polydactyly can be inherited in syndromic and non-syndromic forms. Non-syndromic polydactyly is further classified into Pre-axial, Post-axial, and Meso-axial polydactyly.

In the current study, two Pakistani families with Post-axial polydactyly phenotype, segregating in an autosomal dominant and recessive form are described. One family is consanguineous and the other is non-consanguineous. These families resided in the KP and Sindh province of Pakistan. Blood samples were acquired from both afflicted and unaffected family members for DNA extraction and further analysis. WES

followed by conventional DNA Sanger sequencing was performed to identify the potential disease-causing variants. All four members of family A were undergone WES to finalize the *FGFR3* (c.1657 G>A; p. Val555Met) as a novel pathogenic missense variant, later which was validated by Sanger DNA Sequencing.

The *FGFR3* gene has total 19 exons, with exons 2-18 encoding 806 amino acid protein products. *FGFR3* is a highly conserved tyrosine kinase receptor, mapped on chromosome 4p16.3. This gene comprises three main regions, including an extracellular region composed of three main immunoglobulin domains, an intracellular tyrosine kinase domain, and a transmembrane hydrophobic domain. The protein's external part interacts with fibroblast growth factors *(FGFs)*, which initiates a cascade of signals that ultimately affect cell growth and differentiation. The *FGF* receptor signaling cascade appears to influence p38 MAPK, SAPK/JNK, PI3K, ERK1/2, and PKC pathways, which have all been linked to regulating Mesenchymal stem cell (MSC) differentiation (Ascione et al., 2023). Mutated *FGFR3* have been reported to cause several clinical disorders like platyspondylic lethal skeletal dysplasia, Crouzon syndrome, Pfeiffer syndrome, achondroplasia, hypochondroplasia, and LADD syndrome (Bueno et al., 1999; Rohmann et al., 2006). There is no previously reported mutation of *FGFR3* in post-axial polydactyly.

Family B consisted of two affected members and two normal members out of which one affected member proceeded for WES and 5 genes were shortlisted; *SMO, RAB25, CFAP57, TMPPE,* and, *CZIB*. Sanger sequencing showed no segregation of *RAB25* in a family. *SMO, CFAP57, TMPPE* and *CZIB* were segregated and confirmed by Sanger Sequencing. *CFAP57, TMPPE* and *CZIB* are not previously linked to Polydactyly, while *SMO* (c.1792 G>A; p. Gly598Arg) is a recurrent gene linked to a Postaxial Polydactyly, with a novel homozygous missense variant due to which it was selected as a potential variant responsible for the disease phenotype.

The Smoothened *(SMO)* is a seven-transmembrane receptor protein located on chromosome 7q32.1. The *SMO* protein has three main domains which consist of 787 amino acids. These domains include an extracellular domain (ECD) at the N-terminal end that is made up of a cysteine-rich domain (CRD), a linker domain, a hinge domain, and a membrane-spanning domain (7-TM). The ECD includes amino acid 1

to 200, while the 7-TM domain contains amino acid 221 to 558. The C-terminal end of the protein consists of a cytoplasmic domain that spans from amino acid 559 to 787 (Zhang *et al.,* 2017). The variant is located at the cytoplasmic tail of *SMO*. *SMO* is a main transcription factor of the Sonic Hedgehog (SHh) pathway. Any mutation in the *SMO* leads to disruption of digit patterning. Somatic and germline variants in *SMO* can cause diseases such as Curry–Jones syndrome (CRJS), sporadic basal cell carcinoma (BCC), medulloblastoma (MB), Pallister-Hall-like syndrome and Postaxial polydactyly (PAP) (Fan et al., 2022). In the current study, all affected individuals manifested isolated PAP suggesting that *SMO* can cause syndromic as well as isolated postaxial polydactyly.

In conclusion in the present research work, two novel missense variants were identified in both Pakistani postaxial polydactyly families. These findings will help in the better understanding of mechanisms involved in limb patterning, limb development, and limb deformities. Identification of pathogenic variants will help us in the better understanding of genotype-phenotype correlation and enables prenatal testing of genetic disorders. It is highly beneficial to promote gene-specific treatments, gene therapies, and clinical trials as they have the potential to significantly improve the quality of life for patients. These innovative approaches to healthcare allow for targeted treatment of specific genes, which can lead to more effective and precise medical interventions. By supporting these cutting-edge therapies, we can help ensure that patients receive the best possible care and outcomes. Whole Exome Sequencing was used to swiftly achieve the objectives of human genetic research endeavor in the current study. Further research is required to elucidate the phenotypic and pathophysiological roles of *FGFR3* and *SMO* mutations in genetic dysp

Chapter 5
REFERENCES

REFERENCES

Abbas, S., Khan, H., Alam, Q., Mahmood, A., & Umair, M. (2023). Genetic advances in skeletal disorders: an overview. Journal of Biochemical and Clinical Genetics, 6(1), 57-57.

Aguirre, W. E., Walker, K., & Gideon, S. (2014). Tinkering with the axial skeleton: vertebral number variation in ecologically divergent threespine stickleback populations. Biological Journal of the Linnean Society, 113(1), 204-219.

Ahmad, S., Ali, M. Z., Muzammal, M., Mir, F. A., & Khan, M. A. (2022). The molecular genetics of human appendicular skeleton. Molecular Genetics and Genomics, 297(5), 1195-1214.

Ahmad Z, Liaqat R, Palander O, Bilal M, Zeb S, Ahmad F, Jawad Khan M, Umair M. (2023). Genetic overview of postaxial polydactyly: updated classification. Clinical Genetics, 103(1), 3-15.

Alexander, P. G., & Tuan, R. S. (2010). Role of environmental factors in axial skeletal dysmorphogenesis. Birth Defects Research Part C: Embryo Today: Reviews, 90(2), 118-132.

Ascione CM, Napolitano F, Esposito D, Servetto A, Belli S, Santaniello A, Scagliarini S, Crocetto F, Bianco R, Formisano L. (2023). Role of FGFR3 in bladder cancer: Treatment landscape and future challenges. Cancer Treatment Reviews, 102530.

Baldridge, D., Shchelochkov, O., Kelley, B., & Lee, B. (2010). Signaling pathways in human skeletal dysplasias. Annual review of genomics and human genetics, 11, 189-217.

Ballhause TM, Jiang S, Baranowsky A, Brandt S, Mertens PR, Frosch KH, Yorgan T, Keller J. (2021). Relevance of Notch signaling for bone metabolism and regeneration. International journal of molecular sciences, 22(3), 1325.

Bennett, R. L., French, K. S., Resta, R. G., & Doyle, D. L. (2008). Standardized human pedigree nomenclature: update and assessment of the recommendations

of the National Society of Genetic Counselors. Journal of genetic counseling, 17, 424-433.

Blottner, D., Salanova, M., Püttmann, B., Schiffl, G., Felsenberg, D., Buehring, B., & Rittweger, J. (2006). Human skeletal muscle structure and function preserved by vibration muscle exercise following 55 days of bed rest. European journal of applied physiology, 97, 261-271.

Boilly, B., Vercoutter-Edouart, A., Hondermarck, H., Nurcombe, V., & Le Bourhis, X. (2000). FGF signals for cell proliferation and migration through different pathways. Cytokine & Growth Factor Reviews, 11(4), 295-302.

Bubshait, D. K. (2022). A review of polydactyly and its inheritance: Connecting the dots. Medicine, 101(50), e32060.

Capdevila, J., & Belmonte, J. C. I. (2001). Patterning mechanisms controlling vertebrate limb development. Annual review of cell and developmental biology, 17(1), 87-132.

Chien, S., Tsai, C., Liu, S., Huang, C., Lin, T., Yang, Y., & Tang, C. (2020). Noggin Inhibits IL-1β and BMP-2 Expression, and Attenuates Cartilage Degeneration and Subchondral Bone Destruction in Experimental Osteoarthritis. Cells, 9(4), 927.

de Crombrugghe, B., Lefebvre, V., & Nakashima, K. (2001). Regulatory mechanisms in the pathways of cartilage and bone formation. Current opinion in cell biology, 13(6), 721-728.

Erlebacher, A., Filvaroff, E. H., Gitelman, S. E., & Derynck, R. (1995). Toward a molecular understanding of skeletal development. Cell, 80(3), 371-378.

Estrada-Cuzcano A, Etard C, Delvallée C, Stoetzel C, Schaefer E, Scheidecker S, Geoffroy V, Schneider A, Studer F, Mattioli F, Chennen K. (2020). Novel IQCE variations confirm its role in postaxial polydactyly and cause ciliary defect phenotype in zebrafish. Human Mutation, 41(1), 240-254.

Fan, L., Jin, P., Qian, Y., Shen, G., Shen, X., & Dong, M. (2022). Case report: Prenatal diagnosis of postaxial polydactyly with Bi-allelic variants in smoothened (SMO). Frontiers in Genetics, 13, 887082.

Galjaard RJ, Smits A, Tuerlings JH, Bais AG, Avella AM, Breedveld G, Graaff ED, Oostra BA, Heutink P. (2003). A new locus for postaxial polydactyly type A/B on chromosome 7q21–q34. European Journal of Human Genetics, 11(5), 409-415.

Holmes LB, Nasri H, Hunt AT, Toufaily MH, Westgate MN. (2018). Polydactyly, postaxial, type B. Birth defects research, 110(2), 134-141.

Holstein, T. W. (2012). The evolution of the Wnt pathway. Cold Spring Harbor Perspectives in Biology, 4(7), a007922.

Hong M, Schachter KA, Jiang G, Krauss RS. (2012). Neogenin regulates Sonic Hedgehog pathway activity during digit patterning. Developmental Dynamics, 241(3), 627-637.

Huelsken J, Behrens J. (2002). The Wnt signalling pathway. Journal of cell science, 115(21), 3977-3978.

Johnson RL, Tabin CJ. (1997). Molecular models for vertebrate limb development. Cell, 90(6), 979-990.

Kalsoom UE, Klopocki E, Wasif N, Tariq M, et al. Whole exome sequencing identified a novel zinc-finger gene ZNF141 associated with autosomal recessive postaxial polydactyly type A. J Med Genet. 2013;50(1):47- 53. doi: 10.1136/jmedgenet-2012-101219.

Kornak U, Mundlos S. Genetic disorders of the skeleton: a developmental approach. Am J Hum Genet. 2003 Sep;73(3):447-74. doi: 10.1086/377110. Epub 2003 Jul 31. PMID: 12900795; PMCID: PMC1180673.

Krakow D, Rimoin DL. (2010). The skeletal dysplasias. Genetics in Medicine, 12(6), 327-341.

Kyriazis Z, Kollia P, Grivea I, Stefanou N, Sotiriou S, Dailiana ZH. (2023). Polydactyly: Clinical and molecular manifestations. World Journal of Orthopedics, 14(1), 13-22.

Lefebvre, V., & Bhattaram, P. (2010). Vertebrate skeletogenesis. Current topics in developmental biology, 90, 291-317.

Lettice LA, Heaney SJ, Purdie LA, Li L, de Beer P, Oostra BA, Goode D, Elgar G, Hill RE, de Graaff E. (2003). A long-range Shh enhancer regulates expression in the developing limb and fin and is associated with preaxial polydactyly. Human Molecular Genetics, 12(14), 1725-1735.

L'Hôte CG, Knowles MA. (2005). Cell responses to FGFR3 signalling: growth, differentiation and apoptosis. Experimental cell research, 304(2), 417-431.

Lin W, Klein J. (2021). Recent progress in cartilage lubrication. Advanced Materials, 33(18), 2005513.

Lopez-Rios J. (2016, January). The many lives of SHH in limb development and evolution. In Seminars in cell & developmental biology (Vol. 49, pp. 116-124). Academic Press.

Malik S, Ullah S, Afzal M, Lal K, Haque S. (2014). Clinical and descriptive genetic study of polydactyly: a Pakistani experience of 313 cases. Clinical genetics, 85(5), 482-486.

Manske MC, Kennedy CD, Huang JI (2017). Classifications in brief: the Wassel classification for radial polydactyly. Clinical Orthopaedics and Related Research®, 475, 1740-1746.

Massagué J, Chen YG. (2000). Controlling TGF-β signaling. Genes & development, 14(6), 627-644.

Mead TJ, YutzeyKE. (2009). Notch pathway regulation of chondrocyte differentiation and proliferation during appendicular and axial skeleton development. Proceedings of the National Academy of Sciences, 106(34), 14420-14425.

Rimoin DL, Cohn D, Krakow D, Wilcox W, Lachman RS, Alanay Y. (2007). The skeletal dysplasias: clinical–molecular correlations. Annals of the New York Academy of Sciences, 1117(1), 302-3

Riobo NA, Saucy B, DiLizio C, Manning DR. (2006). Activation of heterotrimeric G proteins by Smoothened. Proceedings of the National Academy of Sciences, 103(33), 12607-12612.

Rohmann E, Brunner HG, Kayserili H, Uyguner O, Nürnberg G, Lew ED, Dobbie A, Eswarakumar VP, Uzumcu A, Ulubil-Emeroglu M, Leroy JG. (2006). Mutations in different components of FGF signaling in LADD syndrome. Nature genetics, 38(4), 414-417.

Salhotra A, Shah HN, Levi B, Longaker MT. (2020). Mechanisms of bone development and repair. Nature Reviews Molecular Cell Biology, 21(11), 696-711.

Savarirayan R, Rimoin DL. (2002). The skeletal dysplasias. Best practice & research Clinical endocrinology & metabolism, 16(3), 547-560.

Schlessinger J, Plotnikov AN, Ibrahimi OA, Eliseenkova AV, Yeh BK, Yayon A, Linhardt RJ, Mohammadi M. (2000). Crystal structure of a ternary FGF-FGFR-heparin complex reveals a dual role for heparin in FGFR binding and dimerization. Molecular cell, 6(3), 743-750.

Schrauwen I, Giese AP, Aziz A, Lafont DT, Chakchouk I, Santos-Cortez RL, Lee K, Acharya A, Khan FS, Ullah A, Nickerson DA. (2019). FAM92A Underlies Nonsyndromic Postaxial Polydactyly in Humans and an Abnormal Limb and Digit Skeletal Phenotype in Mice. Journal of Bone and Mineral Research, 34(2), 375-386.

Taichman RS. (2005). Blood and bone: two tissues whose fates are intertwined to create the hematopoietic stem-cell niche. Blood, 105(7), 2631-2639.

Teven CM, Farina EM, Rivas J, Reid RR. (2014). Fibroblast growth factor (FGF) signaling in development and skeletal diseases. Genes & diseases, 1(2), 199-213.

Ullah A, Nevado J, Yıldırım R, Unal E, Ciorraga M, Barruz P, Chico L, Piceci-Sparascio F, Guida V, De Luca A. (2017). GLI1 inactivation is associated with developmental phenotypes overlapping with Ellis–van Creveld syndrome. Human Molecular Genetics, 26(23), 4556-4571.

Ullah A, Umair M, Majeed AI, Abdullah, Jan A, Ahmad W. (2019). A novel homozygous sequence variant in GLI1 underlies first case of autosomal recessive pre-axial polydactyly. Clinical Genetics, 95(4), 540-541.

Umair M, Ahamd F, Bilal M, Asiri A, Younus M, Khan A. (2019). A comprehensive review of genetic skeletal disorders reported from Pakistan: a brief commentary. Meta Gene, 20, 100559.

Umair M, Ahmad F, Bilal M, Ahmad W, Alfadhel M. (2018). Clinical genetics of polydactyly: an updated review. Frontiers in genetics, 9, 447.09.

Umair M, Palander O, Bilal M, Almuzzaini B, Alam Q, Ahmad F, Younus M, Khan A, Waqas A, Rafeeq MM, Alfadhel M. (2021). Biallelic variant in DACH1, encoding Dachshund Homolog 1, defines a novel candidate locus for recessive postaxial polydactyly type A. Genomics, 113(4), 2495-2502.

Umair M, Shah K, Alhaddad B, Haack TB, Graf E, Strom TM, Meitinger T, Ahmad W. (2017). Exome sequencing revealed a splice site variant in the IQCE gene underlying post-axial polydactyly type A restricted to lower limb. European Journal of Human Genetics, 25(8), 960-965.

Umm-e-Kalsoom, Sulman Basit, Syed Kamran-ul-Hassan Naqvi, Muhammad Ansar, and Wasim Ahmad. 2012. “Genetic Mapping of an Autosomal Recessive Postaxial Polydactyly Type A to Chromosome 13q13.3– Q21.2 and Screening of the Candidate Genes.” Human Genetics 131(3):415–22. doi: 10.1007/s00439-011- 1085-7.

Unger S, Ferreira CR, Mortier GR, Ali H, Bertola DR, Calder A, Cohn DH, Cormier-Daire V, Girisha KM, Hall C, Krakow D. (2023). Nosology of genetic skeletal disorders: 2023 revision. American Journal of Medical Genetics Part A, 191(5), 1164-1209.

Verma PK., El-Harouni AA. (2015). Review of literature: genes related to postaxial polydactyly. Frontiers in pediatrics, 3, 8.

Wang S, Zhao Y, Richardson K, Yang R, Bousraou Z, Fasciano S. (2022). Notch Signaling and Fluid Shear Stress in Regulating Osteogenic Differentiation. bioRxiv, 2022-07.

Waldmann L, Leyhr J, Zhang H, Allalou A, Öhman-Mägi C, Haitina T. (2022). The role of Gdf5 in the development of the zebrafish fin endoskeleton. Developmental Dynamics, 251(9), 1535-1549.

Wan M, Cao X. (2005). BMP signaling in skeletal development. Biochemical and biophysical research communications, 328(3), 651-657.

Xavier GM, Seppala M, Barrell W, Birjandi AA, Geoghegan F, Cobourne MT. (2016). Hedgehog receptor function during craniofacial development. Developmental Biology, 415(2), 198-215.

Yamada S, Taketomi T, Yoshimura A. (2004). Model analysis of difference between EGF pathway and FGF pathway. Biochemical and Biophysical Research Communications, 314(4), 1113-1120.

Zelzer E, Olsen BR. (2003). The genetic basis for skeletal diseases. Nature, 423(6937), 343-348.

Zhang X, Yang J, Li Y, Liu Y. (2005). Both Sp1 and Smad participate in mediating TGF-β1-induced HGF receptor expression in renal epithelial cells. American Journal of Physiology-Renal Physiology, 288(1), F16-F26.

Zhang X, Zhao F, Wu Y, Yang J, Han GW, Zhao S, Ishchenko A, Ye L, Lin X, Ding K, Dharmarajan V. (2017). Crystal structure of a multi-domain human smoothened receptor in complex with a super stabilizing ligand. Nature communications, 8(1), 15383.

Zhao H, Tian Y, Breedveld G, Huang S, Zou Y, Chai J, Li H, Li M, Oostra BA, Lo WH, Heutink P.. (2002). Postaxial polydactyly type A/B (PAP-A/B) is linked to chromosome 19p13. 1-13.2 in a Chinese kindred. European Journal of Human Genetics, 10(3), 162-166.

Search for Disease-Causing Variants in Families with Postaxial Polydactyly Using Whole Exome Sequencing

ORIGINALITY REPORT

10%	5%	8%	2%
SIMILARITY INDEX	INTERNET SOURCES	PUBLICATIONS	STUDENT PAPERS

PRIMARY SOURCES

1	Submitted to Higher Education Commission Pakistan Student Paper	1%
2	Zaheer Ahmad, Romana Liaqat, Oliva Palander, Muhammad Bilal, Shah Zeb, Farooq Ahmad, Muhammad Jawad Khan, Muhammad Umair. "Genetic overview of postaxial polydactyly: Updated classification", Clinical Genetics, 2022 Publication	1%
3	prr.hec.gov.pk Internet Source	1%
4	Lihong Fan, Pengzhen Jin, Yeqing Qian, Guosong Shen, Xueping Shen, Minyue Dong. "Case Report: Prenatal Diagnosis of Postaxial Polydactyly With Bi-Allelic Variants in Smoothened (SMO)", Frontiers in Genetics, 2022 Publication	1%